Report No.
UCB/SEMM-2018/04

Structural Engineering
Mechanics and Materials

A fully-relaxed variationally-consistent framework for inelastic micro-sphere models: Finite viscoelasticity

By

Sanjay Govindjee, Miklos J. Zoller, and Klaus Hackl

April 2018

Department of Civil and Environmental Engineering
University of California, Berkeley

A fully-relaxed variationally-consistent framework for inelastic micro-sphere models: Finite viscoelasticity

Sanjay Govindjee[a,*], Miklos J. Zoller[a], Klaus Hackl[b]

[a] *Structural Engineering, Mechanics, and Materials; Department of Civil and Environmental Engineering; University of California, Berkeley; Berkeley CA 94720-1710, USA*
[b] *Lehrstuhl für Allgemeine Mechanik; Ruhr-Universität Bochum; D-44801 Bochum, Germany*

Abstract

The micro-sphere modeling framework provides a popular means by which one-dimensional mechanical models can easily and quickly be generalized into three-dimensional stress-strain models. The essential notion of the framework, similar to homogenization theory, is that one allows the microstructural kinematic fields to relax subject to a constraint connected to a macroscopic deformation measure. In its standard presentation, the micro-sphere modeling framework is strictly applicable to elastic materials. Presentations considering inelastic phenomena invariably, and inconsistently, assume an affine relation between inelastic macroscopic and microscopic phenomena. In this work we present a methodology by which one can lift this modeling restriction. In particular, we show how one can construct and apply a homogenized Biot theory to generate fully-relaxed variationally-consistent macroscopic models for inelastic materials within the context of the micro-sphere model. The primary application example will be finite deformation viscoelasticity.

Keywords: micro-sphere, finite deformation viscoelasticity

1. Introduction

The development of material models of polymeric materials, elastomers in particular, generally follows either a phenomenological track or a micromechanical one. Common successful phenomenological models include, for example, the two-parameter model of Mooney (1940), Rivlin (1948), and Rivlin and Saunders (1951), the principal stretch model of Ogden (1972, 1984), or the multi-parameter model of Yeoh (1993). While successful, these models lack a direct connection to the microstructural origins of the mechanical response. Models that attempt to address this issue include the famous 3-, 4-, and 8-chain models

*Corresponding author.
Email addresses: s_g@berkeley.edu (Sanjay Govindjee), zollermi@berkeley.edu (Miklos J. Zoller), klaus.hackl@rub.de (Klaus Hackl)

proposed, respectively, by James and Guth (1943), Flory and Rehner (1943), and Arruda and Boyce (1993). This category of models also includes the full network models of Treloar and Riding (1979) and Wu and van der Giessen (1993); see also Puso (1994) for a review of these models.

Underlying these latter micromechanical models is a statistical mechanics model for the force-extension relation for a single polymer chain and an imaginative idealization of the topology of the cross-linked polymer network. These models also employ an affine kinematic assumption, the exception being the 4-chain model of Flory and Rehner (1943) which allows the central tetrahedral junction to take up an energetically relaxed position. The remainder of the models, the affine ones, are essentially homogenization models of a particular network arrangement employing a Taylor (1938)-like kinematic condition (see also Zienkiewicz et al., 2014, Chap. 7) – all the network junctions move affinely with respect to the macroscopic deformation (gradient).

Similar to the full network models is the *micro-plane* model of Bažant and Gambarova (1984) that was developed for the modeling of the fracture of brittle materials; see also Bažant and Oh (1985) and Carol et al. (2004) among other papers from the same group. The micro-plane model starts with a one-dimensional model (inelastic) and then proposes a virtual work equivalence between macroscopic and microscopic virtual work on a spherical representation of the material microstructure. To close the model, an affine kinematic assumption is made between the macroscopic deformation measure and the microstructural deformation measures. The framework of the micro-plane models is one that is clearly connected to the notions of homogenization in the spirit of Hill (1972) and others, but omitting gradient fields due to the point nature of the representative volume element in the micro-plane model.

The *micro-sphere* model by Miehe et al. (2004) improved on these earlier works by recognizing that the full network models were in fact like homogenization models, and it was not necessary to impose an affine assumption on the microstructural kinematics. Rather it was possible to allow the stretch in each direction on the micro-sphere to energetically relax, subject to a macroscopic constraint that keeps the p-root average of the local micro-sphere stretches equal to the p-root average of the affine stretches over the micro-sphere. Strikingly, Miehe et al. (2004) were able to show that this minimization problem had a closed-form solution for single chain models with arbitrary complexity. The micro-sphere modeling framework has been widely used in many contexts. In particular, researchers have extended its use to the case where the underlying chain model is no longer elastic; see e.g. Miehe and Göktepe (2005); Dal and Kaliske (2009); Mistry and Govindjee (2014); Guilié et al. (2015) among others. Unfortunately in these extensions, researchers have had to abandon the fully variational setting developed by Miehe et al. (2004) when treating the inelastic phenomena – the macroscopic and microscopic inelastic evolutions are always connected affinely. It is the goal of this paper to show how to lift this restriction and arrive at a model which includes micromechanical evolution that generates variationally relaxed macroscopic evolution of the inelastic phenomena. To keep the presentation compact, we will restrict ourselves to the case of viscoelasticity.

Similar to the viscoelastic extension by Miehe and Göktepe (2005) we will utilize the dissipation potential concept of Biot (1955). But here we will present a construction that generates a macroscopic dissipation potential from microscopic dissipation potentials at the "chain-level". The methodology employed will be in direct analogy to how macroscopic free energies are constructed from microscopic ones. Thus this work aims to generalize the non-affine homogenization scheme for the determination of the macroscopic free energy in the presence of internal evolutionary phenomena. Viscoelastic behavior will be incorporated through an exploitation of the variational framework of Biot (1955) and an additional relaxation process. Ultimately, this formulation permits the modeling of a wide variety of inelastic polymer behaviors. Following the micro-sphere developments of Tkachuk and Linder (2012) and the micro-plane developments, by for example, Carol et al. (2004), we will additionally utilize tensorial constraints for the micro-sphere relaxation. In the examples, we will do this using the Hencky strain measure as well as the deformation gradient.

2. Preliminaries

We consider deformable continuum bodies with a deformation χ that maps reference points $\boldsymbol{X}$ to current locations $\boldsymbol{x} = \chi(\boldsymbol{X})$. The deformation gradient will be denoted $\boldsymbol{F} = \partial \boldsymbol{x}/\partial \boldsymbol{X}$, the right Cauchy-Green deformation tensor $\boldsymbol{C} = \boldsymbol{F}^T\boldsymbol{F} = \boldsymbol{U}^2$, where $\boldsymbol{U}$ is the right stretch tensor computed from the polar decomposition of $\boldsymbol{F}$; see e.g. Ogden (1984) or Gurtin (1981). Additionally, since $\boldsymbol{C}$ is symmetric and positive definite, by the spectral decomposition theorem:

$$\boldsymbol{C} = \boldsymbol{U}^2 = \sum_{i=1}^{3} \lambda_i^2 \boldsymbol{N}_i \otimes \boldsymbol{N}_i \,,$$

and

$$\boldsymbol{U} = \sum_{i=1}^{3} \lambda_i \boldsymbol{N}_i \otimes \boldsymbol{N}_i \,,$$

where λ_i and $\boldsymbol{N}_i$ are the principal stretches and directions, respectively. The Hencky strain (see Hencky, 1928) can then be expressed as

$$\ln(\boldsymbol{U}) = \sum_{i=1}^{3} \ln(\lambda_i)\, \boldsymbol{N}_i \otimes \boldsymbol{N}_i \,.$$

We further define the volume preserving parts of $\boldsymbol{F}$ and $\boldsymbol{C}$, where $J = \det(\boldsymbol{F})$, by

$$\begin{aligned} \bar{\boldsymbol{F}} &= J^{-1/3}\boldsymbol{F}\,, \\ \bar{\boldsymbol{C}} &= \bar{\boldsymbol{F}}^T\bar{\boldsymbol{F}} = J^{-2/3}\boldsymbol{C}\,. \end{aligned}$$

For one of the viscoelastic models developed below we will additionally adopt the Sidoroff (1974) multiplicative decomposition of the deformation gradient into elastic and inelastic parts:

$$\boldsymbol{F} = \boldsymbol{F}^{\mathrm{E}} \boldsymbol{F}^{\mathrm{V}} ;$$

see also Le Tallec and Rahier (1994); Reese and Govindjee (1998).

3. Fully variational microsphere for viscoelastic materials

This section will focus on generalizing the minimization technique of the micro-sphere model with tensorial constraints. The core of the model is a minimization on micro-scale kinematic variables subject to a constraint enforcing that the continuum deformation is equal to the directional integral average of the microscopic deformation. Additionally, Biot's principle will be utilized to determine the evolution law of the system at the continuum level with the use of a dissipation potential. This approach allows for extension to other evolutionary microstructural phenomena but this will not be the topic of this work.

The micro-sphere model proposed by Miehe et al. (2004) and Miehe and Göktepe (2005) postulates that the topology of the polymer network can be characterized by a micro-sphere. The micro-sphere is composed of a distribution of polymer chains that all connect to the center of the micro-sphere and whose other ends are distributed on the surface of the sphere, S. More generally one can think of tubes of material connecting the center to the surface of the sphere. To each point on the sphere we will define the outward unit normal to be $\boldsymbol{n}$, this gives the orientation of the individual chains/tubes of material. The 3-, 4-, 8-chain, and full network models are included in this framework by assuming either a distribution function composed of 3-, 4-, or 8-Dirac masses or as a uniform ($1/|S| \equiv 1/4\pi$) distribution.

To each point on the sphere we postulate a micro-scale tensorial deformation measure that depends on micro-scale kinematic fields on the surface of the sphere. Example micro-scale kinematic fields that can be used to build such tensor fields would include, for example, the local stretch (Miehe et al., 2004) and the local transverse tube strain for each orientation (Edwards and Vilgis, 1988). The micro-scale kinematic fields need not be scalar (Tkachuk and Linder, 2012). To be more concrete, we assume that for each orientation $\boldsymbol{n}$ there is an associated tensorial micro-scale strain measure $\boldsymbol{E}_{\mathrm{m}}$ that depends on these micro-scale kinematic fields. The subscript m will be used to denote micro-scale variables; corresponding macroscopic quantities will not have the subscript. Furthermore, we will denote by α_i the elastic micro-scale fields on the sphere. To account for inelastic processes, we will also define viscous strain measure $\boldsymbol{E}_{\mathrm{m}}^{\mathrm{V}}$ to model time dependent relaxation phenomena. $\boldsymbol{E}_{\mathrm{m}}^{\mathrm{V}}$ will depend on a different set of micro-scale fields β_j over the sphere.

3.1. The elastic case

As a specialization, and to fix ideas in the simplest possible case, we will briefly review the elastic micro-sphere case in the setting just described. For concreteness let us define the micro-scale “right-stretch tensor” as

$$\boldsymbol{U}_{\mathrm{m}}(\lambda,\nu) = \lambda \boldsymbol{n}\otimes\boldsymbol{n} + \nu(\mathbf{1} - \boldsymbol{n}\otimes\boldsymbol{n})\,,$$

where λ and ν are the local stretch and tube contraction of the material oriented at $\boldsymbol{n}$. This is the primary kinematic assumption on the local deformation. We further introduce the micro-scale Hencky strain as

$$\ln \boldsymbol{U}_{\mathrm{m}} = \frac{1}{3}\ln j\mathbf{1} + 3\ln\xi\left(\boldsymbol{n}\otimes\boldsymbol{n} - \frac{1}{3}\mathbf{1}\right)\,,$$

where the micro-jacobian $j = \lambda\nu^2$ and the micro-deviatoric stretch $\xi = \sqrt[3]{\lambda/\nu}$. In the general notation $\ln\boldsymbol{U}_{\mathrm{m}}$ corresponds to $\boldsymbol{E}_{\mathrm{m}}$, and $\ln j$ and $\ln\xi$ correspond to α_1 and α_2.

The second ingredient of the micro-sphere model is a micro-scale description of the free energy of the material oriented in the direction $\boldsymbol{n}$ in terms of the micro-scale kinematic fields. In the present case, this could be an additively split function

$$\psi_{\mathrm{m}}(\ln j, \ln\xi) = \psi_{\mathrm{m}}^{\mathrm{vol}}(\ln j) + \psi_{\mathrm{m}}^{\mathrm{dev}}(\ln\xi)\,,$$

though other choices are certainly possible. Note, however, that the choices are not fully arbitrary. In particular, Carol et al. (2004) have shown for the micro-plane model that certain choices lead to restrictions on material response that do not comport with usual expectations – such as materials with only negative Poisson’s ratios or fixed Poisson’s ratios (in the small strain limit). These issues also hold true for the micro-sphere model, but the choice given above does not suffer from these defects.

For the present choices, the macroscopic free energy density is then postulated to be given by the energetic relaxation

$$\Psi(\ln\boldsymbol{U}) = \inf_{\ln j, \ln\xi}\left\{\frac{1}{|S|}\int_S \psi_{\mathrm{m}}(\ln j, \ln\xi)\, dS\right\}\,, \tag{1}$$

subject to the kinematic constraint

$$\ln\boldsymbol{U} = \frac{1}{|S|}\int_S \ln\boldsymbol{U}_{\mathrm{m}}\, dS\,. \tag{2}$$

The minimization in (1) subject to (2) can be carried out to generate an elastic stress-strain model, where the Lagrange multiplier used to enforce the constraint is the conjugate stress to $\ln\boldsymbol{U}$; we leave out the details to avoid duplication later. In general the resulting model requires quadrature over the sphere – a point that we will also discuss later. Depending on the choices for the micro-energy densities explicit or implicit models may be obtained. Written in this way, the micro-sphere model is clearly seen to be a type of homogenization model, albeit one that can be computed without having to consider gradient constraints as appear in typical representative volume element homogenization problems.

3.2. The viscoelastic case: General structure

We now return to the general viscoelastic case where in addition to $\boldsymbol{E}_{\mathrm{m}}$ and α_i $(i = 1, \ldots, n_\alpha)$, we also have micro-scale viscous fields $\boldsymbol{E}_{\mathrm{m}}^{\mathrm{V}}$ and β_j $(j = 1, \ldots, n_\beta)$. As with the elastic case, to each micro-scale tensor field we will have a corresponding macro-scale tensor which we will require to be equal to its directional/surface average:

$$\boldsymbol{E} = \frac{1}{|S|} \int_S \boldsymbol{E}_{\mathrm{m}} \left(\alpha_i\right) \, dS \,, \tag{3}$$

$$\boldsymbol{E}^{\mathrm{V}} = \frac{1}{|S|} \int_S \boldsymbol{E}_{\mathrm{m}}^{\mathrm{V}} \left(\beta_j\right) \, dS \,. \tag{4}$$

With the constraints introduced, the macroscopic free energy is constructed through the relaxation of the micro-scale fields α_i and β_j in terms of an energy function ψ_{m} defined for each spatial direction over the micro-sphere,

$$\Psi = \inf_{\alpha_i, \beta_j} \left\{ \frac{1}{|S|} \int_S \psi_{\mathrm{m}} \left(\alpha_i, \beta_j\right) \, dS \right\} \tag{5}$$

subject to (3) and (4).

We solve this optimization problem using two Lagrange multipliers $\boldsymbol{\tau}$ and $\boldsymbol{\tau}^{\mathrm{V}}$ to enforce these constraints via the Lagrangian

$$\begin{aligned} \mathcal{L}\left(\alpha_i, \beta_j, \boldsymbol{\tau}, \boldsymbol{\tau}^{\mathrm{V}}\right) &= \frac{1}{|S|} \int_S \psi_{\mathrm{m}} \left(\alpha_i, \beta_j\right) \, dS \\ &+ \boldsymbol{\tau} : \left[\boldsymbol{E} - \frac{1}{|S|} \int_S \boldsymbol{E}_{\mathrm{m}} \left(\alpha_i\right) \, dS \right] \\ &+ \boldsymbol{\tau}^{\mathrm{V}} : \left[\boldsymbol{E}^{\mathrm{V}} - \frac{1}{|S|} \int_S \boldsymbol{E}_{\mathrm{m}}^{\mathrm{V}} \left(\beta_j\right) \, dS \right] . \end{aligned}$$

The stationary conditions for this Lagrangian yield:

$$\delta_{\alpha_i} \mathcal{L} = \frac{1}{|S|} \int_S \left(\frac{\partial \psi_{\mathrm{m}}}{\partial \alpha_i} - \boldsymbol{\tau} : \frac{\partial \boldsymbol{E}_{\mathrm{m}}}{\partial \alpha_i} \right) \delta\alpha_i \, dS = 0 \,, \tag{6}$$

$$\delta_{\beta_j} \mathcal{L} = \frac{1}{|S|} \int_S \left(\frac{\partial \psi_{\mathrm{m}}}{\partial \beta_j} - \boldsymbol{\tau}^{\mathrm{V}} : \frac{\partial \boldsymbol{E}_{\mathrm{m}}^{\mathrm{V}}}{\partial \beta_j} \right) \delta\beta_j \, dS = 0 \,, \tag{7}$$

$$\delta_{\boldsymbol{\tau}} \mathcal{L} = \delta\boldsymbol{\tau} : \left[\boldsymbol{E} - \frac{1}{|S|} \int_S \boldsymbol{E}_{\mathrm{m}} \left(\alpha_i\right) \, dS \right] = 0 \,, \tag{8}$$

$$\delta_{\boldsymbol{\tau}^{\mathrm{V}}} \mathcal{L} = \delta\boldsymbol{\tau}^{\mathrm{V}} : \left[\boldsymbol{E}^{\mathrm{V}} - \frac{1}{|S|} \int_S \boldsymbol{E}_{\mathrm{m}}^{\mathrm{V}} \left(\beta_j\right) \, dS \right] = 0 \,. \tag{9}$$

Thus, the Euler-Lagrange equations are:

$$\left(\frac{\partial \psi_{\mathrm{m}}}{\partial \alpha_i} - \boldsymbol{\tau} : \frac{\partial \boldsymbol{E}_{\mathrm{m}}}{\partial \alpha_i} \right) = 0 \,, \tag{10}$$

$$\left(\frac{\partial \psi_{\mathrm{m}}}{\partial \beta_j} - \boldsymbol{\tau}^{\mathrm{V}} : \frac{\partial \boldsymbol{E}_{\mathrm{m}}^{\mathrm{V}}}{\partial \beta_j} \right) = 0 \,, \tag{11}$$

along with two macroscopic residual equations enforcing the constraints:

$$\left[\boldsymbol{E} - \frac{1}{|S|}\int_S \boldsymbol{E}_{\mathrm{m}}\left(\alpha_i\right)\, dS\right] \quad = \quad 0\,, \tag{12}$$

$$\left[\boldsymbol{E}^{\mathrm{V}} - \frac{1}{|S|}\int_S \boldsymbol{E}^{\mathrm{V}}_{\mathrm{m}}\left(\beta_j\right)\, dS\right] \quad = \quad 0\,. \tag{13}$$

In general, the free energy ψ_{m} couples the variables α_i and β_j in a nonlinear way, requiring equations (10) and (11) be solved via an iterative method. When done so, the fields α_i and β_j are given in terms of the macro-scale Lagrange multipliers $\boldsymbol{\tau}$ and $\boldsymbol{\tau}^{\mathrm{V}}$, which are straightforwardly shown to be the macroscopic stresses conjugate to $\boldsymbol{E}$ and $\boldsymbol{E}^{\mathrm{V}}$; viz. $\boldsymbol{\tau} = \partial\Psi/\partial\boldsymbol{E}$ and $\boldsymbol{\tau}^{\mathrm{V}} = \partial\Psi/\partial\boldsymbol{E}^{\mathrm{V}}$ (see Appendix A). When the solution fields for α_i and β_j are inserted into (12) and (13), one obtains the micro-sphere's macroscopic stress-strain model (strain in terms of stress). Missing, however, to this point is a rational means for determining the evolution of the macroscopic viscous quantities.

To proceed further we postulate the existence of a micro-scale dissipation potential $\Delta_{\mathrm{m}}(\beta_j, \dot{\beta}_j)$ in the sense of Biot (1955) such that the inelastic micro-field evolution is governed by the minimization problem:

$$\inf_{\dot{\beta}_j}\left[\dot{\psi}_{\mathrm{m}} + \Delta_{\mathrm{m}}\right]\,. \tag{14}$$

In this framework, satisfaction of second law requirements is relatively easy. For example, all functions Δ_{m} that are non-negative homogenous of degree n in the second argument will work. Note that for economy of presentation, we will assume henceforth that Δ_{m} is only a function of $\dot{\beta}_j$.

The main postulate of our work is that a macroscopic dissipation potential Δ can be constructed from an additional relaxation process on the microscopic dissipation potential Δ_{m} in terms of the rate of the viscous internal variables $\dot{\beta}_j$:

$$\Delta = \inf_{\dot{\beta}_j}\left\{\frac{1}{|S|}\int_S \Delta_{\mathrm{m}}\left(\dot{\beta}_j\right)\, dS\right\}\,, \tag{15}$$

subject to the constraint:

$$\dot{\boldsymbol{E}}^{\mathrm{V}} = \frac{1}{|S|}\int_S \overline{\boldsymbol{E}^{\mathrm{V}}_{\mathrm{m}}\left(\beta_j\right)}^{\,\cdot}\, dS\,. \tag{16}$$

And further that the macroscopic evolution then satisfies the macroscopic version of (14):

$$\inf_{\dot{\boldsymbol{E}}^{\mathrm{V}}}\left[\dot{\Psi} + \Delta\right]\,. \tag{17}$$

To determine the macroscopic dissipation potential, we can employ a third Lagrange multiplier $\boldsymbol{\tau}^{\mathrm{d}}$ to enforce equation (16):

$$\begin{aligned}\mathcal{L}\left(\dot{\beta}_j, \boldsymbol{\tau}^{\mathrm{d}}\right) \quad &= \quad \frac{1}{|S|}\int_S \Delta_{\mathrm{m}}\left(\dot{\beta}_j\right)\, dS \\ &+ \quad \boldsymbol{\tau}^{\mathrm{d}} : \left[\dot{\boldsymbol{E}}^{\mathrm{V}} - \frac{1}{|S|}\int_S \overline{\boldsymbol{E}^{\mathrm{V}}_{\mathrm{m}}\left(\beta_j\right)}^{\,\cdot}\, dS\right]\,.\end{aligned}$$

The resulting variational equations yield:

$$\delta_{\dot{\beta}_j}\mathcal{L} = \frac{1}{|S|}\int_S \left(\frac{\partial \Delta_{\mathrm{m}}}{\partial \dot{\beta}_j} - \boldsymbol{\tau}^{\mathrm{d}} : \frac{\partial \dot{\overline{\boldsymbol{E}^{\mathrm{V}}(\beta_j)}}}{\partial \dot{\beta}_j} \right) \delta\dot{\beta}_j \, dS = 0\,, \tag{18}$$

$$\delta_{\boldsymbol{\tau}^{\mathrm{d}}}\mathcal{L} = \delta\boldsymbol{\tau}^{\mathrm{d}} : \left[\dot{\boldsymbol{E}}^{\mathrm{V}} - \frac{1}{|S|}\int_S \dot{\overline{\boldsymbol{E}^{\mathrm{V}}_{\mathrm{m}}(\beta_j)}} \, dS \right] = 0\,. \tag{19}$$

Satisfaction of equation (18) requires

$$\left(\frac{\partial \Delta_{\mathrm{m}}}{\partial \dot{\beta}_j} - \boldsymbol{\tau}^{\mathrm{d}} : \frac{\partial \dot{\overline{\boldsymbol{E}^{\mathrm{V}}(\beta_j)}}}{\partial \dot{\beta}_j} \right) = 0\,, \tag{20}$$

whose solution furnishes the evolution equation for the viscous micro-fields with the macroscopic Lagrange multiplier $\boldsymbol{\tau}^{\mathrm{d}}$ supplying the driving force. When this solution is substituted into (16), one arrives at the macroscopic evolution equation for $\dot{\boldsymbol{E}}^{\mathrm{V}}$.

Examining the governing equations up to this point we see that we have three macroscopic residual equations (3), (4), and (16); further, there are three microscopic residual equations (10), (11), and (20) that allow one to evaluate the macroscopic residuals in terms of the Lagrange mulitpliers. However, macroscopically there are four tensors to be determined by the constitutive framework ($\boldsymbol{E}^{\mathrm{V}}, \boldsymbol{\tau}, \boldsymbol{\tau}^{\mathrm{V}}, \boldsymbol{\tau}^{\mathrm{d}}$), assuming that $\boldsymbol{E}$ is given, and thus one additional macroscopic equation is required. The last equation is furnished by the macroscopic form of Biot's principle (17), leading to:

$$\frac{\partial \Psi}{\partial \boldsymbol{E}^{\mathrm{V}}} + \frac{\partial \Delta}{\partial \dot{\boldsymbol{E}}^{\mathrm{V}}} = 0 \qquad \Rightarrow \qquad \boldsymbol{\tau}^{\mathrm{V}} + \boldsymbol{\tau}^{\mathrm{d}} = 0$$

and the closure of the system of equations. Note that in this setting (16) together with (20) provide the evolution equations for the viscous (internal) variables, and Biot's principle in this setting provides the inter-relation between the Lagrange multipliers. It should also be further noted that if quadratic potentials are chosen, and $\boldsymbol{E}$ and $\boldsymbol{E}^{\mathrm{V}}$ are taken as the total and viscous infinitesimal strain tensors, respectively, then closed form solutions are easily found and the theory of linear viscoelasticity is exactly recovered; see Appendix B.

3.3. Time incremental form

Due to the complexity of the system of constitutive equations, they, like most inelastic models, are often evaluated in a time incremental fashion. The time incremental equations can be derived as shown above where time derivatives are replaced by difference approximations. This methodology follows closely the ideas pioneered by Ortiz and Stainier (1999); Ortiz et al. (2000); Carstensen et al. (2002), and analyzed by Mielke (2004). In what follows, we will use subscripts n and $n+1$ to denote quantities evaluated at times t_n and $t_{n+1} =$

$t_n + h$, where $h > 0$ denotes the time step. In this setting, all quantities at time t_n are assumed known, as is $\boldsymbol{E}_{n+1}$.

The time incremental form of the equations starts by discretizing the expression for the macroscopic dissipation potential (15) as:

$$\Delta\left(\frac{\boldsymbol{E}^{\mathrm{V}}_{n+1} - \boldsymbol{E}^{\mathrm{V}}_{n}}{h}\right) = \inf_{\beta_{j,n+1}} \left\{ \frac{1}{|S|} \int_S \Delta_{\mathrm{m}}\left(\frac{\beta_{j,n+1} - \beta_{j,n}}{h}\right) dS\,, \right\}$$

subject to the time incremental constraint

$$\frac{\boldsymbol{E}^{\mathrm{V}}_{n+1} - \boldsymbol{E}^{\mathrm{V}}_{n}}{h} = \frac{1}{|S|} \int_S \frac{\boldsymbol{E}^{\mathrm{V}}_{m}(\beta_{j,n+1}) - \boldsymbol{E}^{\mathrm{V}}_{m}(\beta_{j,n})}{h}\, dS\,. \tag{21}$$

Constructing the Lagrangian for this problem, one arrives at the time incremental Euler-Lagrange equations

$$D\Delta\left(\frac{\beta_{j,n+1} - \beta_{j,n}}{h}\right) - \boldsymbol{\tau}^{\mathrm{d}} : \frac{\partial \boldsymbol{E}^{\mathrm{V}}_{m,n+1}}{\partial \beta_{j,n+1}} = 0\,,$$

which furnishes the time incremental evolution equation for the micro-scale inelastic fields. Note the operator D indicates differentiation with respect to the function's entire argument.

As with the time continuous case, we employ the macroscopic version of Biot's principle to close the system of equations – this time in its time incremental form. Thus we require

$$\inf_{\boldsymbol{E}^{\mathrm{V}}_{n+1}} \left[\Psi_{n+1}\left(\boldsymbol{E}_{n+1}, \boldsymbol{E}^{\mathrm{V}}_{n+1}\right) - \Psi_{n}\left(\boldsymbol{E}_{n}, \boldsymbol{E}^{\mathrm{V}}_{n}\right) + h \cdot \Delta\left(\boldsymbol{E}^{\mathrm{V}}_{n+1}, \boldsymbol{E}^{\mathrm{V}}_{n}\right)\right]. \tag{22}$$

As before this relation informs us that $\boldsymbol{\tau}^{\mathrm{V}} = -\boldsymbol{\tau}^{\mathrm{d}}$.

4. Nonlinear viscoelasticity with Hencky measures

To illustrate the application of the general theory, we now consider its application to the case of a material that can be modeled using Hencky strain measures. To begin, we postulate at the microstructural level that the chain deformation is described via a tensor, $\boldsymbol{U}_{\mathrm{m}} = \lambda \boldsymbol{n} \otimes \boldsymbol{n} + \nu\,(\mathbf{1} - \boldsymbol{n} \otimes \boldsymbol{n})$, where λ is the chain stretch, ν is the stretch tranverse to the chain, and $\boldsymbol{n}$ is the unit chain orientation vector. As is common in elastomer models, we wish to decouple these variables into volumetric and isochoric components. This is achieved by first defining a micro-jacobian $j = \lambda\nu^2$ and a purely deviatoric kinematic variable $\xi = \sqrt[3]{\lambda/\nu}$. From here we can define the isochoric part of the micro-strain tensor:

$$\bar{\boldsymbol{U}}_{\mathrm{m}} = j^{-1/3}\boldsymbol{U}_{\mathrm{m}} = \xi^2 \boldsymbol{n} \otimes \boldsymbol{n} + \xi^{-1}(\mathbf{1} - \boldsymbol{n} \otimes \boldsymbol{n})\,,$$

or equivalently

$$\boldsymbol{U}_{\mathrm{m}} = j^{1/3}\bar{\boldsymbol{U}}_{\mathrm{m}} = j^{1/3}\xi^2 \boldsymbol{n} \otimes \boldsymbol{n} + j^{1/3}\xi^{-1}(\mathbf{1} - \boldsymbol{n} \otimes \boldsymbol{n})\,.$$

The strain measure we will use will be the Hencky (logarithmic) strain:

$$\ln \boldsymbol{U}_{\mathrm{m}} = \frac{1}{3} \ln j \mathbf{1} + 3 \ln \xi \, \mathbb{D}(\boldsymbol{n}) \, ,$$

where $\mathbb{D}(\boldsymbol{n}) = \boldsymbol{n} \otimes \boldsymbol{n} - \frac{1}{3}\mathbf{1}$. The viscous micro-strain will be assumed to be purely deviatoric and thus to have the following form:

$$\ln \boldsymbol{U}_m^V = \sum_{i=1}^{n} 3 \ln \xi_i^{\mathrm{V}} \, \mathbb{D}(\boldsymbol{n}) \, . \tag{23}$$

The factor of 3 in front of the $\ln \xi_i^{\mathrm{V}}$ terms is used for convenience. The parameter n in the summation above denotes how many viscous relaxation terms are needed to accurately represent a particular material's mechanical response. For simplicity of presentation we will assume $n = 1$ and drop the summation.

For the micro-scale free energy we will assume an additive structure with equilibrium and non-equilibrium terms and one that also splits deviatoric from volumetric contributions:

$$\psi_{\mathrm{m}}(\ln j, \ln \xi, \ln \xi_i^{\mathrm{V}}) = \psi_{\mathrm{m}}^{\mathrm{vol,eq}}(\ln j) + \psi_{\mathrm{m}}^{\mathrm{dev,eq}}(\ln \xi) + \psi_{\mathrm{m}}^{\mathrm{dev,neq}}(\ln \xi, \ln \xi^{\mathrm{V}}) \, .$$

Setting up the free energy Lagrangian with Lagrange multipliers $\boldsymbol{\tau}$ and $\boldsymbol{\tau}^{\mathrm{V}}$, we have:

$$\begin{aligned} \mathcal{L}\left(\ln j, \ln \xi, \ln \xi^{\mathrm{V}}, \boldsymbol{\tau}, \boldsymbol{\tau}^{\mathrm{V}}\right) &= \frac{1}{|S|} \int_S \psi_{\mathrm{m}}\left(\ln j, \ln \xi, \ln \xi^{\mathrm{V}}\right) dS \\ + \boldsymbol{\tau} : \left[\ln \boldsymbol{U} - \frac{1}{|S|} \int_S \ln \boldsymbol{U}_{\mathrm{m}} dS\right] &+ \boldsymbol{\tau}^{\mathrm{V}} : \left[\ln \boldsymbol{U}^{\mathrm{V}} - \frac{1}{|S|} \int_S \ln \boldsymbol{U}_{\mathrm{m}}^{\mathrm{V}} dS\right] . \end{aligned}$$

Here $\ln \boldsymbol{U}$ represents the total macroscopic Hencky strain and $\ln \boldsymbol{U}^{\mathrm{V}}$ represents the macroscopic viscous Hencky strain. The resulting Euler-Lagrange equations are:

$$\frac{\partial \psi_{\mathrm{m}}^{\mathrm{vol,eq}}}{\partial \ln j} - \boldsymbol{\tau} : \frac{1}{3}\mathbf{1} = 0 \, , \tag{24}$$

$$\frac{\partial \psi_{\mathrm{m}}^{\mathrm{dev,eq}}}{\partial \ln \xi} + \frac{\partial \psi_{\mathrm{m}}^{\mathrm{dev,neq}}}{\partial \ln \xi} - \boldsymbol{\tau} : 3 \, \mathbb{D}(\boldsymbol{n}) = 0 \, , \tag{25}$$

$$\frac{\partial \psi_{\mathrm{m}}^{\mathrm{dev,neq}}}{\partial \ln \xi^{\mathrm{V}}} - \boldsymbol{\tau}^{\mathrm{V}} : 3 \, \mathbb{D}(\boldsymbol{n}) = 0 \, , \tag{26}$$

along with the two constraint equations:

$$\ln \boldsymbol{U} - \frac{1}{|S|} \int_S \ln j \frac{1}{3}\mathbf{1} + 3 \ln \xi \, \mathbb{D}(\boldsymbol{n}) \, dS = 0 \, , \tag{27}$$

$$\ln \boldsymbol{U}^{\mathrm{V}} - \frac{1}{|S|} \int_S 3 \ln \xi^{\mathrm{V}} \, \mathbb{D}(\boldsymbol{n}) \, dS = 0 \, . \tag{28}$$

The conjugate stresses, the Lagrange multipliers, are the rotated Kirchhoff stresses; see Hoger (1987).

It is interesting to observe that (24) implies that $\ln j$ is a constant over the micro-sphere. Thus $\ln j$ behaves affinely, $j = J$. This result provides justification for the arbitrary assumption in Miehe et al. (2004) that the energetic relaxation for the micro-sphere construction is only performed on the deviatoric part of the motion. The two other micro-fields $\ln \xi$ and $\ln \xi^{\mathrm{V}}$ are coupled via (25) and (26). If we denote the solution of the equations for the micro-fields with a superposed $*$, then we see that they are a function of $\boldsymbol{\tau}$ and $\boldsymbol{\tau}^{\mathrm{V}}$ and orientation $\boldsymbol{n}$:

$$\ln \xi^{*}(\boldsymbol{\tau}, \boldsymbol{\tau}^{\mathrm{V}}, \boldsymbol{n}) \qquad \text{and} \qquad \ln \xi^{V*}(\boldsymbol{\tau}, \boldsymbol{\tau}^{\mathrm{V}}, \boldsymbol{n}) \qquad \text{and} \qquad \ln j^{*}(\boldsymbol{\tau}) \,,$$

which implies that (27) and (28) become at time t_{n+1}

$$\ln \boldsymbol{U}_{n+1} - \frac{1}{|S|} \int_S \ln j^{*}(\boldsymbol{\tau}) \frac{1}{3} \mathbf{1} + 3 \ln \xi^{*}(\boldsymbol{\tau}, \boldsymbol{\tau}^{\mathrm{V}}, \boldsymbol{n}) \, \mathbb{D}(\boldsymbol{n}) \, dS = 0 \,, \tag{29}$$

$$\ln \boldsymbol{U}^{\mathrm{V}}_{n+1} - \frac{1}{|S|} \int_S 3 \ln \xi^{V*}(\boldsymbol{\tau}, \boldsymbol{\tau}^{\mathrm{V}}, \boldsymbol{n}) \, \mathbb{D}(\boldsymbol{n}) \, dS = 0 \,. \tag{30}$$

To complete the system of equations, we can apply the developments of Sec. 3.3 to the present case. Doing so results in the time incremental relation for the inelastic micro-scale field as

$$D \Delta_{\mathrm{m}} \left(\frac{\ln \xi^{\mathrm{V}}_{n+1} - \ln \xi^{\mathrm{V}}_{n}}{h} \right) + 3 \boldsymbol{\tau}^{\mathrm{V}} : \mathbb{D}(\boldsymbol{n}) = 0 \,, \tag{31}$$

where we have used the macroscopic version of Biot's principle (17) to eliminate the third Lagrange multiplier. If we solve (31) for the inelastic micro-fields and then plug back into the time incremental constraint (21), we find

$$\ln \boldsymbol{U}^{\mathrm{V}}_{n+1} = \ln \boldsymbol{U}^{\mathrm{V}}_{n} + \frac{h}{|S|} \int_S [D \Delta_{\mathrm{m}}]^{-1} \left(-3 \boldsymbol{\tau}^{\mathrm{V}} : \mathbb{D}(\boldsymbol{n}) \right) \, dS \,, \tag{32}$$

as the incremental update formula for the macroscopic inelastic Hencky strains. Equations (29), (30), and (32) constitute the macroscopic constitutive equations for the model. They represent 3 tensor equations in the three unknowns $\ln \boldsymbol{U}^{\mathrm{V}}_{n+1}$, the inelastic strains, $\boldsymbol{\tau}$, the total stress, and $\boldsymbol{\tau}^{\mathrm{V}}$ the viscous stress. (For convenience we have omitted the time step subscript for the stress tensors).

4.1. Numerical Algorithm

The solution to (29), (30), and (32) requires two issues to be addressed when used in the conventional strain driven setting. The first is that the equations are implicit in terms of the stress and thus have to be inverted. This is easily done using a Newton-Raphson iteration. The other numerical issue that arises is that one needs to evaluate integrals on the sphere to compute the terms in the governing equations. This can be achieved by a quadrature, whereby

$$\frac{1}{|S|} \int_S f(x) \, dS \approx \sum_{i=1}^{n_q} f(x_i) w_i \,,$$

where the x_i are the quadrature points, w_i are the weights, and n_q are the number of quadrature points. Recent studies have shown problems with the accuracy and reliability of common numerical integration methods over the sphere. Verron (2015), for example, compares various numerical integration methods for evaluating constitutive equations over the micro-sphere and has concluded that the number of quadrature points for a given scheme is very important in yielding accurate results. However, further work done by Itskov (2016) shows that numerical integration is still a reliable and accurate tool for full network models. A majority of the disagreement seems to be in the smoothness of the functions used. We took this into account and have studied the accuracy of integrating micro-free energies on the micro-sphere for a variety of points and different integration schemes. We omit the details here and simply note that the symmetric 21 point integration rule formulated by Bažant and Oh (1986) provided reasonable accuracy for the moderate levels of finite deformation show below. Good results can also be found with the more expensive rules of Sloan and Womersley (2004), Fliege and Maier (1999), and Freund et al. (2011).

4.2. Comparison to data: Tire derived materials

As an application of the model, we consider the experiments on tire-derived materials (TDMs) from Montella et al. (2016), who showed that Hencky based continuum models were appropriate for such materials. TDMs are made by cold forging a mix of styrene-butadiene rubber fibers from recycled vehicle tires and grains with a polyurethane binder. This results in a material composed of about 90 percent styrene-butadiene fibers and about 10 percent grains with varying densities. In addition, TDMs are compressible, so the original micro-sphere model for nearly incompressible materials will not suffice here. This utilizes the $\ln j$ component of our micro-strain model unlike common rubber elasticity models which inherently assume incompressibility.

We choose to compare our model to a TDM with a density of 500 $\mathrm{kg/m^3}$, excited in uniaxial compression and simple shear at a loading frequency of 0.1 Hz. For the uniaxial compression test, there was a static pre-strain of 10% followed by a superimposed sinusoidal compression varying in amplitude in the range of 1% to 20%. The second test was a dynamic lap-shear test in which the sample specimen was loaded up to 100% shear strain. The reader is referred to Montella et al. (2016) for more details.

Since the authors used a modified version of the exponentiated Hencky strain energy, Neff et al. (2015), we choose to use microscopic potentials with a similar structure, given by (33)–(36). The exponentiated energies are important to achieve proper energy growth at large deformations. Note that the choice of these functions is somewhat arbitrary and any one-dimensional micromechanical model can be employed within the proposed framework. The functions chosen are only intended for illustration purposes. A set of non-optimized material parameters are given in Table 4.2.

$$
\begin{aligned}
\psi_{\mathrm{m}}^{\mathrm{vol,eq}} &= \frac{E_v}{2}(\ln j)^2 && (33)\\
\psi_{\mathrm{m}}^{\mathrm{dev,eq}} &= \frac{E_{d1}}{2}(\ln \xi)^2 + \frac{E_{d2}}{4}(\ln \xi)^4 + \frac{E_{d3}}{2\kappa_1}\exp\left(\kappa_1 (\ln \xi)^2\right) && (34)\\
\psi_{\mathrm{m}}^{\mathrm{dev,neq}} &= \frac{\mu_1}{2}\left(\ln \xi - \ln \xi^{\mathrm{V}}\right)^2 + \frac{\mu_2}{4}\left(\ln \xi - \ln \xi^{\mathrm{V}}\right)^4 \\
&+ \frac{\mu_3}{2\kappa_2}\exp\left(\kappa_2\left(\ln \xi - \ln \xi^{\mathrm{V}}\right)^2\right) && (35)\\
\Delta_{\mathrm{m}} &= \frac{\eta_1}{2}\left(\ln \dot{\xi}^{\mathrm{V}}\right)^2 + \frac{\eta_2}{4}\left(\ln \dot{\xi}^{\mathrm{V}}\right)^4 && (36)
\end{aligned}
$$

E_v (MPa)	E_{d1} (MPa)	E_{d2} (MPa)	E_{d3} (MPa)	κ_1 (-)	μ_1 (MPa)	μ_2 (MPa)	μ_3 (MPa)	κ_2 (-)
0.5	0.215	0.2	0.16	1.18	0.2	0.4	0.55	1.0

η_1 (MPa·s)	η_2 (MPa·s)
0.115	3.25

Table 1: Material parameters for Figures 1 and 2.

Figures 1 and 2 show the results for our model compared to the data for the tire-derived material. The plots of the total stretch $\lambda = j^{1/3}\xi^2$ and the ratio of the total stretch to $\lambda^{\mathrm{V}} = (\xi^{\mathrm{V}})^2$ illustrate that once the macroscopic material response has been computed, the micro-fields are available via function evaluation/post-processing to allow investigation of local effects. For these two loading cases, our model performs reasonably well in simulating the experimental data. We are able to accurately obtain the stress for the largest deformations while still predicting the overall response of the stress-strain curve. However, we do note that the compression stress/strain simulation is not as accurate as in the shear case due to the slightly anisotropic microstructure of the tire derived material. The overall response of the model is, of course, also tightly connected to the quality of the one-dimensional micro-scale potentials used, and we have not attempted to optimize these in this work, as our main focus is on the overall modeling framework.

5. Nonlinear viscoelasticity with a multiplicative split

In this section we illustrate the use of our framework to extend the maximal advance path constraint scheme presented in Tkachuk and Linder (2012) to include viscous relaxation phenomena. The "strain measure" used here will be the deformation gradient $\boldsymbol{F}$. In the spirit of the multiplicative decomposition $\boldsymbol{F} = \boldsymbol{F}^{\mathrm{E}}\boldsymbol{F}^{\mathrm{V}}$ (Sidoroff, 1974), we assume micro-scale elastic and viscous

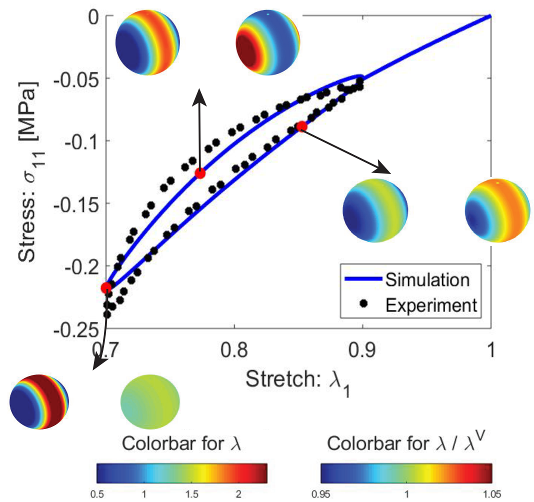

Figure 1: Data from Montella et al. (2016). The left sphere represents the total stretch along various orientations for the micro-sphere, while the right sphere represents the non-equilibirum stretch.

deformation gradients of the form:

$$\boldsymbol{F}_{\mathrm{m}}^{\mathrm{E}} = \alpha \cdot \boldsymbol{n} \otimes \boldsymbol{n}^{\mathrm{V}} , \tag{37}$$
$$\boldsymbol{F}_{\mathrm{m}}^{\mathrm{V}} = \boldsymbol{n}^{\mathrm{V}} \otimes \boldsymbol{n}_0 , \tag{38}$$
$$\boldsymbol{F}_{\mathrm{m}} = \boldsymbol{F}_{\mathrm{m}}^{\mathrm{E}} \boldsymbol{F}_{\mathrm{m}}^{\mathrm{V}} = \boldsymbol{n} \otimes \boldsymbol{n}_0 . \tag{39}$$

Here, the total micro-strain is the outer product of the deformed orientation vector $\boldsymbol{n}$ and the original directional vector $\boldsymbol{n}_0$ over the surface of the sphere; i.e. $\boldsymbol{n}_0$ maps to $\boldsymbol{n}$. We extend Tkachuk and Linder (2012) using a similar kinematic assumption for the viscous micro-scale deformation gradient and introduce a new variable $\boldsymbol{n}^{\mathrm{V}}$ accounting for the mapping of $\boldsymbol{n}_0$ from the reference to intermediate configuration; $\alpha = 1/\|\boldsymbol{n}^{\mathrm{V}}\|$ to ensure that we recover $\boldsymbol{F}_{\mathrm{m}} = \boldsymbol{n} \otimes \boldsymbol{n}_0$ when multiplying $\boldsymbol{F}_{\mathrm{m}}^{\mathrm{E}}$ and $\boldsymbol{F}_{\mathrm{m}}^{\mathrm{V}}$ together.

The requisite constraint equations for the relaxations are now given in terms of the *vectorial* micro-fields $\boldsymbol{n}$ and $\boldsymbol{n}^{\mathrm{V}}$:

$$\frac{1}{3}\boldsymbol{F} = \frac{1}{|S|}\int_S \boldsymbol{F}_{\mathrm{m}}(\boldsymbol{n})\, dS , \tag{40}$$
$$\frac{1}{3}\boldsymbol{F}^{\mathrm{V}} = \frac{1}{|S|}\int_S \boldsymbol{F}_{\mathrm{m}}^{\mathrm{V}}(\boldsymbol{n}^{\mathrm{V}})\, dS . \tag{41}$$

(The factor of $1/3$ as noted in Tkachuk and Linder (2012) is due to the fact that for no deformation $\frac{1}{|S|}\int_S \boldsymbol{n}_0 \otimes \boldsymbol{n}_0 \, dS = \frac{1}{3}\mathbf{1}$.) Continuing with the framework, we again assume a decoupled micro free energy into equilibrium $\psi_{\mathrm{m}}^{\mathrm{eq}}$ and non-equilibrium $\psi_{\mathrm{m}}^{\mathrm{neq}}$ components, where $\psi_{\mathrm{m}}^{\mathrm{eq}}$ will depend on the norm of $\boldsymbol{n}$ and $\psi_{\mathrm{m}}^{\mathrm{neq}}$

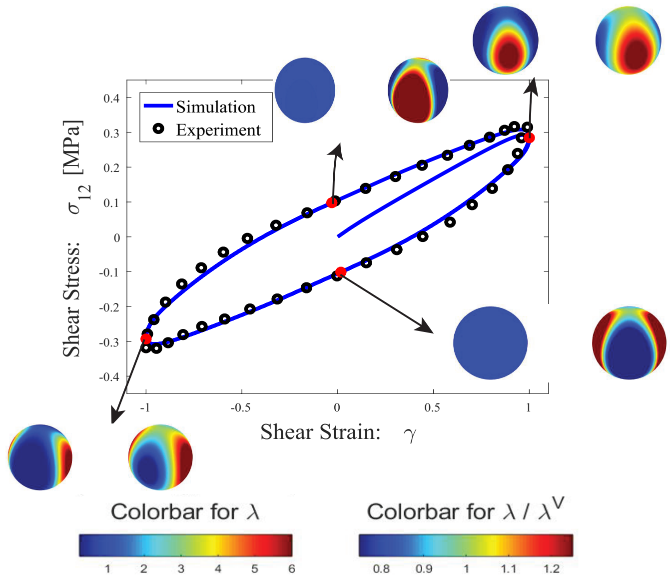

Figure 2: Data from Montella et al. (2016). The left sphere represents the total stretch along various orientations for the micro-sphere, while the right sphere represents the non-equilibrium stretch.

will depend on $||\boldsymbol{n} - \boldsymbol{n}^{\mathrm{V}}||$. Additionally, the microscopic dissipation potential is defined in terms of $||\dot{\overline{\boldsymbol{n}^{\mathrm{V}}}}||$:

$$\begin{aligned} \psi_{\mathrm{m}}(\boldsymbol{n}, \boldsymbol{n}^{\mathrm{V}}) &= \psi_{\mathrm{m}}^{\mathrm{eq}}(||\boldsymbol{n}||) + \psi_{\mathrm{m}}^{\mathrm{neq}}(||\boldsymbol{n} - \boldsymbol{n}^{\mathrm{V}}||)\,, \\ \Delta_{\mathrm{m}}(\dot{\overline{\boldsymbol{n}^{\mathrm{V}}}}) &= \Delta_{\mathrm{m}}(||\dot{\overline{\boldsymbol{n}^{\mathrm{V}}}}||)\,. \end{aligned}$$

The remainder of the model details follow in exactly the same fashion as above. Perhaps the only point of note is that the conjugate stresses that appear in this formulation are 1st Piola-Kirchhoff stress (and they appear as one-third times the Lagrange multipliers).

5.1. Comparison to data: Tire derived materials

As with the Hencky example we will apply this model to the TDM data of Montella et al. (2016). The potential functions chosen, as before, are for illustrative purposes:

$$\psi_{\mathrm{m}}^{\mathrm{eq}} = \frac{E_1}{2}\exp\left(||\boldsymbol{n}||^2\right) + \frac{E_2}{2}||\boldsymbol{n}||^2 + K\left(\log||\boldsymbol{n}||\right)^2\,,$$

$$\psi_{\mathrm{m}}^{\mathrm{neq}} = \frac{\mu}{2}||\boldsymbol{n} - \boldsymbol{n}^{\mathrm{V}}||^2\,,$$

$$\Delta_{\mathrm{m}} = \frac{\eta_1}{2}||\dot{\overline{\boldsymbol{n}^{\mathrm{V}}}}||^2 + \frac{\eta_2}{4}||\dot{\overline{\boldsymbol{n}^{\mathrm{V}}}}||^4\,.$$

The (non-optimized) material parameter used are shown in Table 2.

The model is seen to be able to model large deformations and with large amounts of dissipation. We can see that for roughly the same accuracy as the Hencky model, one needs half as many material parameters with our viscoelastic extension of the maximal advance path constraint structure from Tkachuk and Linder (2012). This highlights the importance of good micro-scale models when using the micro-sphere framework to model materials.

E_1 (MPa)	E_2 (MPa)	K (MPa)	μ (MPa)	η_1 (MPa·s)	η_2 (MPa·s)
0.10	0.10	1.254	10.0	0.10	0.15

Table 2: Material parameters for Figures 3 and 4.

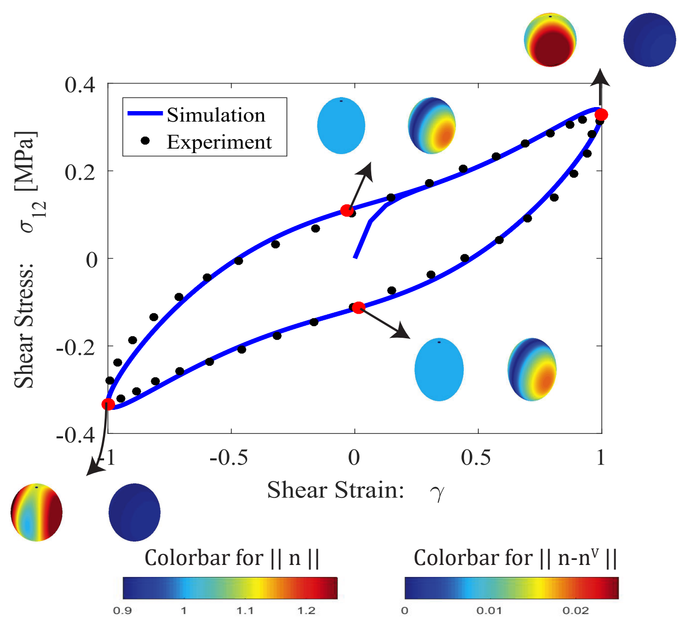

Figure 3: Data from Montella et al. (2016). The left sphere colorbar shows the norm of the elastic vector $\boldsymbol{n}$, while the right sphere colorbar shows the norm of the difference $\boldsymbol{n} - \boldsymbol{n}^{\mathrm{V}}$.

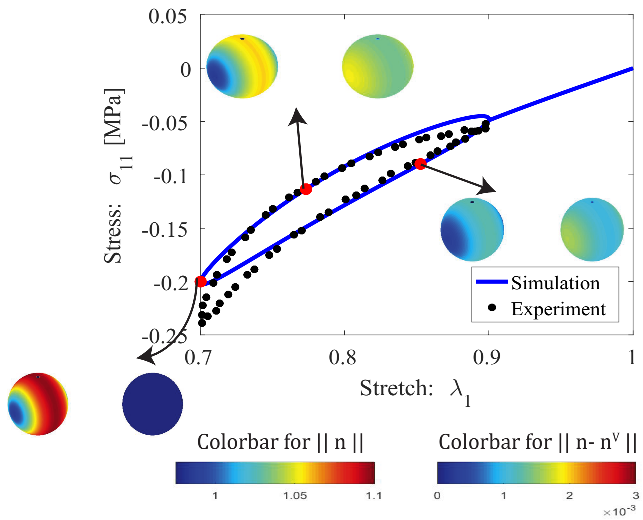

Figure 4: Data from Montella et al. (2016). The left sphere colorbar shows the norm of the elastic vector $\boldsymbol{n}$, while the right sphere colorbar shows the norm of the difference $\boldsymbol{n} - \boldsymbol{n}^{\mathrm{V}}$.

6. Conclusion

The micro-sphere framework is a popular framework for extending one-dimensional elastic models into three dimensions via energetic relaxation of micro-scale energies subject to macro-micro relational constraints. Outside of the elastic case, efforts to date have always relied upon an affine connection between macroscopic and microscopic inelasticity. In this work we have presented a structure for dispensing with this affine assumption.

The construction requires that the micro-scale material response be governed by one-dimensional models that admit a Biot variational representation. In particular we have shown via examples that this applies to linear and non-linear viscoelasticity (at both finite and small deformations). We also note that it applies to many models of plasticity, strain crystallization, and other transformation phenomena.

The key ingredient for removing the affine connection, is the assumption that there exists a macroscopic dissipation potential that can be derived from a variational relaxation of the average of the micro-scale dissipation potential over the micro-sphere. The relaxation is performed subject to macro-micro kinematic constraints. The resulting structure provides a macroscopic three-dimensional evolutionary model for inelastic behavior that is variationally fully consistent with the microscopic material model that one assumes.

While we have applied our relaxation scheme to the micro-sphere, we also note that the idea of constructing macroscopic dissipation potentials from microscopic dissipation potentials applies more generally. In particular, it naturally extends to inelastic composite materials, where one, however, must also deal with the issue gradient constraints should one desire to do better than Voigt averaging.

Bibliography

Arruda, E. and Boyce, M. (1993), 'A three-dimensional constitutive model for the large stretch behavior of rubber elastic materials', *Journal of Mechanics and Physics of Solids* **41**, 389–412.

Bažant, Z. (1988), 'Microplane model for brittle-plastic material: I. Theory', *Journal of Engineering Mechanics* **114**(10), 1672–1687.

Bažant, Z. and Gambarova, P. (1984), 'Crack shear in concrete: Crack band microplane model', *ASCE Journal of Structural Engineering* **100**, 2015–2035.

Bažant, Z. and Oh, B. (1985), 'Microplane model for progressive fracture of concrete and rock', *ASCE Journal of Engineering Mechanics* **111**, 559–582.

Bažant, Z. and Oh, B. (1986), 'Efficient numerical integration on the surface of a sphere', *Journal of Applied Mathematics and Mechanics* **66**, 37–49.

Biot, M. (1955), 'Variational principles in irreversible thermodynamics with application to viscoelasticity', *The Physical Review* **97**, 1463–1469.

Carol, I., Jirásek, M. and Bažant, Z. (2004), 'A framework for microplane models at large strain, with application to hyperelasticity', *International Journal of Solids and Structures* **41**, 511–557.

Carstensen, C., Hackl, K. and Mielke, A. (2002), 'Non–convex potentials and microstructures in finite–strain plasticity', *Proceedings of the Royal Society of London A: Mathematical, Physical and Engineering Sciences* **458**, 299–317.

Dal, H. and Kaliske, M. (2009), 'A micro-continuum-mechanical material model for failure of rubber-like materials: Application to ageing-induced fracturing', *Journal of the Mechanics and Physics of Solids* **57**, 1340 – 1356.

Edwards, S. and Vilgis, T. (1988), 'The tube model theory of rubber elasticity', *Reports on Progress in Physics* **51**, 243–297.

Fliege, J. and Maier, U. (1999), 'The distribution of points on the sphere and corresponding cubature formulate', *IMA Journal of Numerical Analysis* **19**, 317–334.

Flory, P. and Rehner, J. (1943), 'Statisticla mechanics of cross-linked polymer networks. I. Rubberlike elasticity', *Journal of Chemical Physics* **11**, 512–520.

Freund, M., Lorenz, H., Juhre, D., Ihlemann, J. and Klöppel, M. (2011), 'Finite element implementation of a microstructure-based model for filled elastomers', *International Journal of Plasticity* **27**, 902 – 919.

Guilié, J., Le, T.-N. and Le Tallec, P. (2015), 'Micro-sphere model for strain-induced crystallisation and three-dimensional applications', *Journal of the Mechanics and Physics of Solids* **81**, 58 –74.

Gurtin, M. (1981), *An introduction to continuum mechanics*, Academic Press, New York.

Hencky, H. (1928), 'Über die Form des Elastizitätsgesetzes bei ideal elastischen Stoffen', *Zeitschift für Technische Physik* **9**, 215–220.

Hill, R. (1972), 'On constitutive macro-variables for hetrogeneous solids at finite strain', *Proceedings of the Royal Society of London A* **326**, 131–147.

Hoger, A. (1987), 'The stress conjugate to logarithmic strain', *International Journal of Solids and Structures* **23**, 1645–1656.

Itskov, M. (2016), 'On the accuracy of numerical integration over the unit sphere applied to full network models', *Computational Mechanics* **57**, 859–865.

James, H. and Guth, E. (1943), 'Theory of elastic properties of rubber', *Journal of Chemical Physics* **11**, 455–481.

Le Tallec, P. and Rahier, C. (1994), 'Numerical models of steady rolling for non-linear viscoelastic structures in finite deformations', *International Journal for Numerical Methods in Engineering* **37**, 1159–1186.

Miehe, C. and Göktepe, S. (2005), 'A micro-macro approach to rubber-like materials – Part II: The micro-sphere model of finite rubber viscoelasticity', *Journal of Mechanics and Physics of Solids* **53**, 2231–2258.

Miehe, C., Göktepe, S. and Lulei, F. (2004), 'A micro-macro approach to rubber-like materials – Part I: The non-affine micro-sphere model of rubber elasticity', *Journal of the Mechanics and Physics of Solids* **52**, 2617–2660.

Mielke, A. (2004), 'Existence of minimizers in incremental elasto-plasticity with finite strains', *SIAM Journal of Mathematical Analysis* **36**, 384–404.

Mistry, S. J. and Govindjee, S. (2014), 'A micro-mechanically based continuum model for strain-induced crystallization in natural rubber', *International Journal of Solids and Structures* **51**, 530 – 539.

Montella, G., Govindjee, S. and Neff, P. (2016), 'The exponentiated Hencky strain energy in modeling tire derived material for moderately large deformations', *Journal of Engineering Materials and Technology* **138**, 1–12.

Mooney, M. (1940), 'A theory of large elastic deformation', *Journal of Applied Physics* **11**, 582–592.

Neff, P., Ghiba, I.-D. and Lankeit, J. (2015), 'The exponentiated hencky-logarithmic strain energy. part i: Constitutive issues and rank-one convexity', *Journal of Elasticity* **121(2)**, 143–234.

Ogden, R. (1972), 'Large deformation isotropic elasticity: On the correlation of theory and experiment for incompressible rubberlike solids', *Proceedings of the Royal Society of London* **326**, 565–584.

Ogden, R. (1984), *Non-linear Elastic Deformations*, Ellis-Horwood, Chichester England.

Ortiz, M., Repetto, E. and Stanier, L. (2000), 'A theory of subgrain dislocation structures', *Journal of the Mechanics and Physics of Solids* **48**, 2077–2114.

Ortiz, M. and Stainier, L. (1999), 'The variational formulation of viscoplastic constitutive updates', *Computer Methods in Applied Mechanics and Engineering* **171**, 419–444.

Puso, M. (1994), Mechanistic Constitutive Models for Rubber Elasticity and Viscoelasticity, PhD thesis, University of California, Davis. (Available as UCRL-ID-151578, 2003, https://e-reports-ext.llnl.gov/pdf/243854.pdf).

Reese, S. and Govindjee, S. (1998), 'A theory of finite viscoelasticity and numerical aspects', *International Journal of Solids and Structures* **35**, 3455–3482.

Rivlin, R. (1948), 'Large elastic deformations of isotropic materials IV. Further developments of the general theory', *Philosophical Transactions of the Royal Society of London A* **241**, 379–397.

Rivlin, R. and Saunders, D. (1951), 'Large elastic deformations of isotropic materials. VII. Experiments on the deformation of rubber', *Philosophical Transactions of the Royal Society of London A* **243**, 251–288.

Sidoroff, F. (1974), 'Un modèle viscoélastique non linéaire avec configuration intermédiaire', *Journal de Mécanique* **13**, 679–713.

Sloan, I. and Womersley, R. (2004), 'Extremal systems of points and numerical integration on the sphere', *Advances in Computational Mathematics* **21**, 107–125.

Taylor, G. (1938), 'Plastic strain in metals', *Journal of the Institute of Metals* **62**, 307–324.

Tkachuk, M. and Linder, C. (2012), 'The maximal advance path constraint for the homogenization of materials with random network microstructure', *Philosophical Magazine* **92**, 2779–2808.

Treloar, L. and Riding, G. (1979), 'A non-Gaussian theory for rubber in biaxial strain. I. Mechanical properties', *Proceedings of the Royal Society London A* **369**, 261–280.

Verron, E. (2015), 'Questioning numerical integration methods for microsphere (and microplane) constitutive equations', *Mechanics of Materials* **89**, 216–228.

Wu, P. and van der Giessen, E. (1993), 'On improved network models for rubber elasticity and their applications to orientation hardening in glassy polymers', *Journal of the Mechanics and Physics of Solids* **41**, 427–456.

Yeoh, O. (1993), 'Some forms of the strain-energy function for rubber', *Rubber Chemistry and Technology* **66**, 754–771.

Zienkiewicz, O., Taylor, R. and Fox, D. (2014), *The Finite Element Method for Solid and Structural Mechanics*, 7th edn, Butterworth-Heinemann, Waltham MA.

Appendix A. Lagrange multipliers and conjugate stresses

The conjugate stresses to the macroscopic variables are straightforwardly show to be equal to the Lagrange multipliers in our relaxation problems. Consider a micro-scale free energy in terms of a two sets of micro-fields α_i (elastic) and β_j (viscous), subject to averaging constraints, such that the governing Lagrangian is given by

$$\begin{aligned} \mathcal{L}(\alpha_i, \beta_j, \boldsymbol{\tau}, \boldsymbol{\tau}^{\mathrm{V}}) &= \frac{1}{|S|} \int_S \Psi_{\mathrm{m}}(\alpha_i, \beta_j)\, dS \\ &+ \boldsymbol{\tau} : \left[\boldsymbol{E} - \frac{1}{|S|} \int_S \boldsymbol{E}_{\mathrm{m}}(\alpha_i)\, dS \right] \\ &+ \boldsymbol{\tau}^{\mathrm{V}} : \left[\boldsymbol{E} - \frac{1}{|S|} \int_S \boldsymbol{E}^{\mathrm{V}}_{\mathrm{m}}(\beta_j)\, dS \right] \end{aligned}$$

The corresponding stationary conditions yield:

$$\delta_{\alpha_i} \mathcal{L} = \frac{1}{|S|} \int_S \left(\frac{\partial \Psi_{\mathrm{m}}}{\partial \alpha_i} - \boldsymbol{\tau} : \frac{\partial \boldsymbol{E}_{\mathrm{m}}}{\partial \alpha_i} \right) \delta\alpha_i dS = 0 \tag{A.1}$$

$$\delta_{\beta_j} \mathcal{L} = \frac{1}{|S|} \int_S \left(\frac{\partial \Psi_{\mathrm{m}}}{\partial \beta_j} - \boldsymbol{\tau}^{\mathrm{V}} : \frac{\partial \boldsymbol{E}^{\mathrm{V}}_{\mathrm{m}}}{\partial \beta_j} \right) \delta\beta_j dS = 0 \tag{A.2}$$

$$\delta_{\boldsymbol{\tau}} \mathcal{L} = \boldsymbol{E} - \frac{1}{|S|} \int_S \boldsymbol{E}_{\mathrm{m}}(\alpha_i) dS = 0 \tag{A.3}$$

$$\delta_{\boldsymbol{\tau}^{\mathrm{V}}} \mathcal{L} = \boldsymbol{E}^{\mathrm{V}} - \frac{1}{|S|} \int_S \boldsymbol{E}^{\mathrm{V}}_{\mathrm{m}}(\beta_j) dS = 0 \tag{A.4}$$

Taking the derivative of equation (A.3) with respect to $\boldsymbol{E}$ yields:

$$\mathbb{I}^{\mathrm{sym}} - \frac{1}{|S|} \int_S \frac{\partial \boldsymbol{E}_{\mathrm{m}}}{\partial \alpha_i} \frac{\partial \alpha_i}{\partial \boldsymbol{E}}\, dS = 0\,.$$

Taking the derivative of equation (A.4) with respect to $\boldsymbol{E}^{\mathrm{V}}$ yields:

$$\mathbb{I}^{\mathrm{sym}} - \frac{1}{|S|} \int_S \frac{\partial \boldsymbol{E}^{\mathrm{V}}_{\mathrm{m}}}{\partial \beta_j} \frac{\partial \beta_j}{\partial \boldsymbol{E}^{\mathrm{V}}}\, dS = 0\,.$$

It is also useful to note, that by the assumed independence of $\boldsymbol{E}$ and $\boldsymbol{E}^{\mathrm{V}}$:

$$
\begin{aligned}
\mathbf{0} &= \frac{1}{|S|}\int_S \frac{\partial \boldsymbol{E}_{\mathrm{m}}}{\partial \alpha_i}\frac{\partial \alpha_i}{\partial \boldsymbol{E}^{\mathrm{V}}}\,dS \\
\mathbf{0} &= \frac{1}{|S|}\int_S \frac{\partial \boldsymbol{E}^{\mathrm{V}}_{\mathrm{m}}}{\partial \beta_j}\frac{\partial \beta_j}{\partial \boldsymbol{E}}\,dS
\end{aligned}
$$

From (A.1) and (A.2), we have the following Euler-Lagrange equations:

$$
\begin{aligned}
\frac{\partial \Psi_{\mathrm{m}}}{\partial \alpha_i} &= \boldsymbol{\tau} : \frac{\partial \boldsymbol{E}_{\mathrm{m}}}{\partial \alpha_i}\,, \\
\frac{\partial \Psi_{\mathrm{m}}}{\partial \beta_j} &= \boldsymbol{\tau}^{\mathrm{V}} : \frac{\partial \boldsymbol{E}^{\mathrm{V}}_{\mathrm{m}}}{\partial \beta_j}\,.
\end{aligned}
$$

If their solution is denoted by α_i^* and β_j^* then our macroscopic energy becomes:

$$
\Psi\left(\boldsymbol{E}, \boldsymbol{E}^{\mathrm{V}}\right) = \frac{1}{|S|}\int_S \Psi_{\mathrm{m}}(\alpha_i^*, \beta_j^*)\,dS\,.
$$

The conjugate stress will be given by $\partial\Psi/\partial\boldsymbol{E}$ and $\partial\Psi/\partial\boldsymbol{E}^{\mathrm{V}}$.

$$
\begin{aligned}
\frac{\partial \Psi}{\partial \boldsymbol{E}} &= \frac{1}{|S|}\int_S \frac{\partial \Psi_{\mathrm{m}}}{\partial \alpha_i^*}\frac{\partial \alpha_i^*}{\partial \boldsymbol{E}} + \frac{\partial \Psi_{\mathrm{m}}}{\partial \beta_j^*}\frac{\partial \beta_j^*}{\partial \boldsymbol{E}}\,dS \\
&= \frac{1}{|S|}\int_S \boldsymbol{\tau} : \frac{\partial \boldsymbol{E}_{\mathrm{m}}}{\partial \alpha_i^*}\frac{\partial \alpha_i^*}{\partial \boldsymbol{E}} + \boldsymbol{\tau}^{\mathrm{V}} : \frac{\partial \boldsymbol{E}^{\mathrm{V}}_{\mathrm{m}}}{\partial \beta_j^*}\frac{\partial \beta_j^*}{\partial \boldsymbol{E}}\,dS \\
&= \boldsymbol{\tau} : \mathbb{I}^{\mathrm{sym}} + \boldsymbol{\tau}^{\mathrm{V}} : \mathbf{0} \\
&= \boldsymbol{\tau}\,.
\end{aligned}
$$

Similarly, for the viscous conjugate stress:

$$
\begin{aligned}
\frac{\partial \Psi}{\partial \boldsymbol{E}^{\mathrm{V}}} &= \frac{1}{|S|}\int_S \frac{\partial \Psi_{\mathrm{m}}}{\partial \alpha_i^*}\frac{\partial \alpha_i^*}{\partial \boldsymbol{E}^{\mathrm{V}}} + \frac{\partial \Psi_{\mathrm{m}}}{\partial \beta_j^*}\frac{\partial \beta_j^*}{\partial \boldsymbol{E}^{\mathrm{V}}}\,dS \\
&= \frac{1}{|S|}\int_S \boldsymbol{\tau} : \frac{\partial \boldsymbol{E}_{\mathrm{m}}}{\partial \alpha_i^*}\frac{\partial \alpha_i^*}{\partial \boldsymbol{E}^{\mathrm{V}}} + \boldsymbol{\tau}^{\mathrm{V}} : \frac{\partial \boldsymbol{E}^{\mathrm{V}}_{\mathrm{m}}}{\partial \beta_j^*}\frac{\partial \beta_j^*}{\partial \boldsymbol{E}^{\mathrm{V}}}\,dS \\
&= \boldsymbol{\tau} : \mathbf{0} + \boldsymbol{\tau}^{\mathrm{V}} : \mathbb{I}^{\mathrm{sym}} \\
&= \boldsymbol{\tau}^{\mathrm{V}}\,.
\end{aligned}
$$

Appendix B. Linear Viscoelasticity

In the linear case, the strain measure chosen is the infinitesimal strain tensor $\boldsymbol{\varepsilon}$. We assume a microscopic strain tensor, $\boldsymbol{\varepsilon}_{\mathrm{m}} = \boldsymbol{\varepsilon}^{\mathrm{e}}_{\mathrm{m}} + \boldsymbol{\varepsilon}^{\mathrm{v}}_{\mathrm{m}}$, which is decomposed into a total elastic strain and a viscous strain. The micro-scale tensors are constructed from three scalar fields $\varepsilon_{\mathrm{vol}}$, $\varepsilon_{\mathrm{dev}}$, and $\varepsilon^{\mathrm{v}}_{\mathrm{dev}}$ accounting for the total volumetric, total deviatoric, and viscous deviatoric deformations, respectively.

These correspond to α_1, α_2, and β_1 from the general theory. The micro-scale strains are given by:

$$\boldsymbol{\varepsilon}_{\mathrm{m}} = \varepsilon_{\mathrm{vol}}\frac{\mathbf{1}}{3} + \varepsilon_{\mathrm{dev}}\left(\boldsymbol{n}\otimes\boldsymbol{n} - \frac{\mathbf{1}}{3}\right) , \tag{B.1}$$

$$\boldsymbol{\varepsilon}^{\mathrm{v}}_{\mathrm{m}} = \varepsilon^{\mathrm{v}}_{\mathrm{dev}}\left(\boldsymbol{n}\otimes\boldsymbol{n} - \frac{\mathbf{1}}{3}\right) . \tag{B.2}$$

Here we assume that the viscous strain is purely deviatoric and the vector $\boldsymbol{n}$ denotes orientation on the sphere. An alternate micro-strain decomposition is to have $\alpha_1 = \varepsilon_a$ correspond to an axial stretch and $\alpha_2 = \varepsilon_c$ correspond to a transverse contraction. This is similar to the approach in Miehe et al. (2004) and Bažant and Gambarova (1984) leading to:

$$\boldsymbol{\varepsilon}_{\mathrm{m}} = \varepsilon_a \boldsymbol{n}\otimes\boldsymbol{n} + \varepsilon_c\left(\mathbf{1} - \boldsymbol{n}\otimes\boldsymbol{n}\right) , \tag{B.3}$$

$$\boldsymbol{\varepsilon}^{\mathrm{v}}_{\mathrm{m}} = \varepsilon^{\mathrm{v}}_a \boldsymbol{n}\otimes\boldsymbol{n} + \varepsilon^{\mathrm{v}}_c\left(\mathbf{1} - \boldsymbol{n}\otimes\boldsymbol{n}\right) . \tag{B.4}$$

In the setting with axial and transverse micro-fields it is attractive, considering only the elastic case (i.e. no $\boldsymbol{\varepsilon}^{\mathrm{v}}_{\mathrm{m}}$), to have a micro-scale energy of the form $\psi_{\mathrm{m}} = \psi_{m,a}(\varepsilon_a) + \psi_{m,c}(\varepsilon_c)$, where the $\psi_{m,a}$ and $\psi_{m,c}$ are quadratic. However this Ansatz leads to Poisson ratios that are strictly negative for all positive microscopic moduli. The negative values respect the thermodynamic limits of the Poisson ratio being greater than -1, but one is not able to reach positive values. This is not a result of the form of micro-scale strain measure, but due to the postulated structure of the free energy. Since physically these terms are coupled via a Poisson ratio effect, we cannot neglect a coupled free energy term. Therefore, our model utilizes the volumetric and deviatoric kinematic variables so that we are able to obtain the full range of thermodynamically admissible Poisson ratios in the linear elastic case (no viscous phenomena). A similar problem with the Poisson ratio was also seen in the original affine micro-plane model formulated by Bažant and Gambarova (1984), where it was only able to take on values of 0.25 for two-dimesional problems and 1/3 for three-dimensional problems. In the original formulation, only normal and tangential strain components were considered for each micro-plane, which corresponds to equation (B.3). This problem was fixed in Bažant (1988) by considering an additional shear strain on each micro-plane along with decoupling the normal strain into volumetric and deviatoric components; see also Carol et al. (2004).

Continuing, we can employ quadratic potentials for the microscopic free energy and dissipation potential:

$$\psi_{\mathrm{m}} = \frac{1}{2}K\left(\varepsilon_{\mathrm{vol}}\right)^2 + \frac{1}{2}G_{\infty}\left(\varepsilon_{\mathrm{dev}}\right)^2 + \frac{1}{2}G_1\left(\varepsilon_{\mathrm{dev}} - \varepsilon^{\mathrm{v}}_{\mathrm{dev}}\right)^2 \tag{B.5}$$

$$\Delta_{\mathrm{m}} = \frac{1}{2}\eta_G\left(\dot{\varepsilon}^{\mathrm{v}}_{\mathrm{dev}}\right)^2 \tag{B.6}$$

Here K, G_{∞}, and G_1 are the microscopic bulk modulus, equilibrium shear modulus, and viscous shear modulus, respectively; η_G is a microscopic measure of internal viscosity.

Following the procedure outlined in the previous section, the macroscopic free energy is defined as in equation (5) with the corresponding Lagrangian in terms of the micro-kinematic variables and two Lagrange multipliers $\boldsymbol{\tau}$ and $\boldsymbol{\tau}^{\mathrm{v}}$:

$$
\begin{aligned}
&\mathcal{L}(\varepsilon_{\mathrm{vol}},\varepsilon_{\mathrm{dev}},\varepsilon^{\mathrm{v}}_{\mathrm{dev}},\boldsymbol{\tau},\boldsymbol{\tau}^{\mathrm{v}}) = \\
&\qquad \frac{1}{|S|}\int_S \frac{1}{2}K\left(\varepsilon_{\mathrm{vol}}\right)^2 + \frac{1}{2}G_\infty\left(\varepsilon_{\mathrm{dev}}\right)^2 + \frac{1}{2}G_1\left(\varepsilon_{\mathrm{dev}}-\varepsilon^{\mathrm{v}}_{\mathrm{dev}}\right)^2 dS \\
&\qquad + \boldsymbol{\tau} : \left(\boldsymbol{\varepsilon} - \frac{1}{|S|}\int_S \boldsymbol{\varepsilon}_{\mathrm{m}} dS\right) + \boldsymbol{\tau}^{\mathrm{v}} : \left(\boldsymbol{\varepsilon}^{\mathrm{v}} - \frac{1}{|S|}\int_S \boldsymbol{\varepsilon}^{\mathrm{v}}_{\mathrm{m}} dS\right) .
\end{aligned}
$$

As before, we define $\mathbb{D}(\boldsymbol{n}) = \boldsymbol{n}\otimes\boldsymbol{n} - \frac{1}{3}\mathbf{1}$. The stationary conditions yield:

$$
\delta_{\varepsilon_{\mathrm{vol}}}\mathcal{L} = \frac{1}{|S|}\int_S \left[K\varepsilon_{\mathrm{vol}} - \boldsymbol{\tau} : \frac{\mathbf{1}}{3}\right]\delta\varepsilon_{\mathrm{vol}}\, dS = 0\,, \tag{B.7}
$$

$$
\begin{aligned}
\delta_{\varepsilon_{\mathrm{dev}}}\mathcal{L} &= \frac{1}{|S|}\int_S \left[G_\infty(\varepsilon_{\mathrm{dev}}) + G_1(\varepsilon_{\mathrm{dev}}-\varepsilon^{\mathrm{v}}_{\mathrm{dev}}) - \boldsymbol{\tau} : \mathbb{D}(\boldsymbol{n})\right]\delta\varepsilon_{\mathrm{dev}}\, dS \\
&= 0\,,
\end{aligned} \tag{B.8}
$$

$$
\delta_{\varepsilon^{\mathrm{v}}_{\mathrm{dev}}}\mathcal{L} = \frac{1}{|S|}\int_S \left[-G_1(\varepsilon_{\mathrm{dev}}-\varepsilon^{\mathrm{v}}_{\mathrm{dev}}) - \boldsymbol{\tau}^{\mathrm{v}} : \mathbb{D}(\boldsymbol{n})\right]\delta\varepsilon^{\mathrm{v}}_{\mathrm{dev}}\, dS = 0\,, \tag{B.9}
$$

$$
\delta_{\boldsymbol{\tau}}\mathcal{L} = \delta\boldsymbol{\tau} : \left(\boldsymbol{\varepsilon} - \frac{1}{|S|}\int_S \varepsilon_{\mathrm{vol}}\frac{\mathbf{1}}{3} + \varepsilon_{\mathrm{dev}}\mathbb{D}(\boldsymbol{n})\, dS\right) = 0\,, \tag{B.10}
$$

$$
\delta_{\boldsymbol{\tau}^{\mathrm{v}}}\mathcal{L} = \delta\boldsymbol{\tau}^{\mathrm{v}} : \left(\boldsymbol{\varepsilon}^{\mathrm{v}} - \frac{1}{|S|}\int_S \varepsilon^{\mathrm{v}}_{\mathrm{dev}}\mathbb{D}(\boldsymbol{n})\, dS\right) = 0\,. \tag{B.11}
$$

This set of linear equations is easily solved for the micro-kinematic variables in terms of the Lagrange multipliers. If we then plug these results back into the constraint equations, we can solve for the Lagrange multipliers in terms of the macroscopic strains by splitting them into deviatoric and volumetric parts. With this procedure one finds that the macroscopic free energy:

$$
\begin{aligned}
\Psi = \frac{1}{2}3K\boldsymbol{\varepsilon} : \mathbb{I}^{\mathrm{vol}} : \boldsymbol{\varepsilon} + \frac{1}{2}G_\infty\frac{15}{2}\left[\boldsymbol{\varepsilon} : \mathbb{I}^{\mathrm{dev}} : \boldsymbol{\varepsilon}\right] \\
+ \frac{1}{2}G_1\frac{15}{2}\left[(\boldsymbol{\varepsilon}-\boldsymbol{\varepsilon}^{\mathrm{v}}) : \mathbb{I}^{\mathrm{dev}} : (\boldsymbol{\varepsilon}-\boldsymbol{\varepsilon}^{\mathrm{v}})\right]\,,
\end{aligned} \tag{B.12}
$$

where $\mathbb{I} = \mathbb{I}^{\mathrm{dev}} + \mathbb{I}^{\mathrm{vol}}$, $\mathbb{I}^{\mathrm{vol}} = \frac{1}{3}\mathbf{1}\otimes\mathbf{1}$.

The conjugate stresses are the derivatives of the free energy with respect to the strains, yielding:

$$
\begin{aligned}
\boldsymbol{\tau} &= \frac{\partial\Psi}{\partial\boldsymbol{\varepsilon}} = 3K\boldsymbol{\varepsilon} : \mathbb{I}^{\mathrm{vol}} + G_\infty\frac{15}{2}\boldsymbol{\varepsilon} : \mathbb{I}^{\mathrm{dev}} \\
&+ G_1\frac{15}{2}(\boldsymbol{\varepsilon}-\boldsymbol{\varepsilon}^{\mathrm{v}}) : \mathbb{I}^{\mathrm{dev}}\,,
\end{aligned} \tag{B.13}
$$

$$
\boldsymbol{\tau}^{\mathrm{v}} = \frac{\partial\Psi}{\partial\boldsymbol{\varepsilon}^{\mathrm{v}}} = -G_1\frac{15}{2}\left(\boldsymbol{\varepsilon}-\boldsymbol{\varepsilon}^{\mathrm{v}}\right) : \mathbb{I}^{\mathrm{dev}}\,. \tag{B.14}
$$

The evolution of the viscous strain is determined through the use of a dissipation potential. The Lagrangian associated with relaxation problem (15) subject to (16) is given by

$$\mathcal{L}\left(\dot{\varepsilon}^{\mathrm{v}}_{\mathrm{dev}}, \boldsymbol{\tau}^{\mathrm{d}}\right) = \frac{1}{|S|}\int_S \frac{1}{2}\eta_G \left(\dot{\varepsilon}^{\mathrm{v}}_{\mathrm{dev}}\right)^2 dS + \boldsymbol{\tau}^{\mathrm{d}} : \left[\dot{\boldsymbol{\varepsilon}}^{\mathrm{v}} - \frac{1}{|S|}\int_S \dot{\varepsilon}^{\mathrm{v}}_{\mathrm{dev}}\mathbb{D}(\boldsymbol{n})\, dS\right]$$

Following the same procedure above, the resulting variational equations are:

$$\begin{aligned} \delta_{\dot{\varepsilon}^{\mathrm{v}}_{\mathrm{dev}}}\mathcal{L} &= \frac{1}{|S|}\int_S \left[\eta_G \cdot \dot{\varepsilon}^{\mathrm{v}}_{\mathrm{dev}} - \boldsymbol{\tau}^{\mathrm{d}} : \mathbb{D}(\boldsymbol{n})\right] \delta\dot{\varepsilon}^{\mathrm{v}}_{\mathrm{dev}} dS = 0\,, && \text{(B.15)} \\ \delta_{\boldsymbol{\tau}^{\mathrm{d}}}\mathcal{L} &= \delta\boldsymbol{\tau}^{\mathrm{d}} : \left[\dot{\boldsymbol{\varepsilon}}^{\mathrm{v}} - \frac{1}{|S|}\int_S \dot{\varepsilon}^{\mathrm{v}}_{\mathrm{dev}}\mathbb{D}(\boldsymbol{n}) dS\right] = 0\,. && \text{(B.16)} \end{aligned}$$

Solving these linear equations, and plugging back into the expression for the macroscopic dissipation potential, gives the macroscopic dissipation potential as:

$$\Delta = \frac{1}{2}\eta_G \frac{15}{2}\left[\dot{\boldsymbol{\varepsilon}}^{\mathrm{v}} : \mathbb{I}^{\mathrm{dev}} : \dot{\boldsymbol{\varepsilon}}^{\mathrm{v}}\right]\,. \tag{B.17}$$

Again it is easily shown that the conjugate stress to the dissipation potential is the new Lagrange multiplier,

$$\boldsymbol{\tau}^{\mathrm{d}} = \frac{\partial \Delta}{\partial \dot{\boldsymbol{\varepsilon}}^{\mathrm{v}}} = \eta_G \frac{15}{2}\dot{\boldsymbol{\varepsilon}}^{\mathrm{v}} : \mathbb{I}^{\mathrm{dev}}\,. \tag{B.18}$$

Combining equations (B.12) and (B.17) with the Biot framework will determine the evolution equation of the system:

$$\inf_{\dot{\boldsymbol{\varepsilon}}^{\mathrm{v}}}\left[\dot{\Psi}(\boldsymbol{\varepsilon}, \boldsymbol{\varepsilon}^{\mathrm{v}}) + \Delta(\dot{\boldsymbol{\varepsilon}}^{\mathrm{v}})\right]\,,$$

or equivalently,

$$\begin{aligned} \frac{\partial \Psi}{\partial \boldsymbol{\varepsilon}^{\mathrm{v}}} + \frac{\partial \Delta}{\partial \dot{\boldsymbol{\varepsilon}}^{\mathrm{v}}} &= 0\,, && \text{(B.19)} \\ \boldsymbol{\tau}^{\mathrm{v}} + \boldsymbol{\tau}^{\mathrm{d}} &= 0\,. && \text{(B.20)} \end{aligned}$$

Substituting these relations back into the equation above:

$$\dot{\boldsymbol{\varepsilon}}^{\mathrm{v}} - \frac{G_1}{\eta_G}\left(\boldsymbol{\varepsilon} - \boldsymbol{\varepsilon}^{\mathrm{v}}\right) : \mathbb{I}^{\mathrm{dev}} = 0\,. \tag{B.21}$$

Considering (B.13) and (B.21), we see we have exactly the macroscopic model for the standard linear solid when one identifies K as the macroscopic bulk modulus, $\frac{15}{2}G_\infty$ as the macroscopic equilibrium modulus, $\frac{15}{2}G_1$ as the macroscopic non-equilibrium modulus, and $\frac{15}{2}\eta_G$ as the macroscopic viscosity.

Appendix C. Surface Integrals

For the derivations in Appendix B, the following results are helpful to know:

$$\frac{1}{|S|}\int_{S^2} \boldsymbol{n}\otimes\boldsymbol{n}\,dS = \frac{1}{3}\mathbf{1}\,,$$

$$\frac{1}{|S|}\int_{S^2} \boldsymbol{n}\otimes\boldsymbol{n}\otimes\boldsymbol{n}\otimes\boldsymbol{n}\,dS = \frac{1}{15}\left(\mathbf{1}\otimes\mathbf{1}+2\mathbb{I}^{\text{sym}}\right)\,,$$

and

$$\frac{1}{|S|}\int_{S} \mathbb{D}(\boldsymbol{n})\otimes\mathbb{D}(\boldsymbol{n})dS = \frac{2}{15}\mathbb{I}^{\text{dev}}\,.$$